

On-line monitoring and quantification of a process reaction by near-infrared spectroscopy. Catalysed esterification of butan-1-ol by acetic acid

Marcelo Blanco and Daniel Serrano

Department Chemistry, Analytical Chemistry Unit, Faculty of Science, Autònoma University of Barcelona, E-08193, Bellaterra, Barcelona, Spain. E-mail: marcel.blanco@uab.es

Received 23rd June 2000, Accepted 21st September 2000

First published as an Advance Article on the web 26th October 2000

The acid-catalysed esterification of butan-1-ol by acetic acid was monitored and quantified using near-infrared spectroscopy (NIRS). Partial least-squares regression (PLSR) was used to construct calibration models based on synthetic mixtures of the esterification components (*viz.* butan-1-ol, acetic acid, *n*-butyl acetate and water) with a view to determining all of them simultaneously. The constructed models were used to monitor a set of esterification reactions based on a factorial design using initial composition and temperature as factors; the results thus obtained were consistent with those provided by the GC reference method, even for reactions performed at higher temperatures than those used for calibration, with relative standard error of prediction (RSEP) values less than 3.5% in all cases. The kinetics of the reaction were calculated and it was shown that the reaction follows theoretical second-order kinetics, which is expected for this esterification. The proposed method allows one to determine quantitatively rate constants, end-points, yields and equilibrium constants, and also the influence of initial water on the performance of the reaction. A statistical study of these variables, based on the characteristics of the used experimental design, proved that the studied factors and their interaction were significant, and that higher temperatures and an excess of acetic acid were the best conditions. The proposed NIR method is thus an effective alternative to traditional methods and is suitable for the on-line quantitative control of batch processes.

Introduction

Obtaining high quality products which can compete in a global market makes it necessary to change and modernize analytical process control techniques. Instrumental techniques capable of making fast acquisition of analytical information, which should be correctly treated to obtain the relevant information that will be used to take decisions, are needed. Nowadays, industry is focused on implementing on-line methods that control directly the parameters of interest in an industrial process, which is in itself a challenging problem that the analyst should solve. A better control of industrial batch processes, such as of processes performed continuously, is important and is finding increasing applications in the chemical, pharmaceutical, petrochemical, alimentary and biotechnical industries among many others.¹ The procedures in batch processes are relatively simple; basically, the reactants are loaded into the reaction vessel, processed under controlled conditions and then the completed product is discharged. Their advantage is their ability to produce high-value products within short manufacturing times. Variations from batch to batch should be minimised as much as possible. In continuous processes, the analytes of interest are always present in the reaction media and the main goal is to keep them in well-defined concentration ranges. The usual way of obtaining information from them is by performing at-line analysis from aliquots taken from the process.

Any kind of industrial process is complex in nature due, mainly, to its multicomponent nature. Thus, even with extensive automation, control of industrial processes is very challenging. Industry is rapidly moving away from at-line and post-production investigation due to its wastefulness both of resources and time.²

A more active approach for industrial processes is to develop an on-line methodology that is capable of monitoring chemical changes throughout the process within the reaction vessel, with a view to controlling the process from a remote position. This

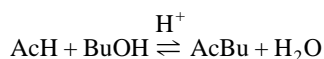
calls for the use of an *in situ* probe or a flow cell that conveys data to a spectrophotometer. Such data, when analysed with chemometric techniques, offer information vital to the modelling step.

Models for monitoring a dynamic process are usually constructed by withdrawing samples from the system of interest and analysing them using reference methods;³ the results from the different species in such samples and the spectral information obtained from them are used to construct calibration models. In this work, however, we used a more simple and convenient approach involving the use of a set of externally prepared samples to construct calibration models. In this way, the need to collect samples for analysis was avoided, sample preparation was facilitated, the whole concentration range spanned by each component throughout the process was encompassed and high correlation among analytes, characteristic when using reacting samples, was avoided.

Over the past decade near-infrared spectroscopy (NIRS) has evolved rapidly and has become the technique of choice for food analyses,⁴ in addition to being a highly useful tool for pharmaceutical,⁵ petrochemical⁶ and biomedical tests,⁷ among others. This technique is simple and non-destructive, requires no sample pre-treatment and is very rapid, all of which makes it suitable for quality control analyses. Notwithstanding its high potential, NIRS has scarcely been used for the on-line control of industrial process. Some published applications of NIRS in remote monitoring include fermentation analysis,⁸ the petrochemical industry,⁹ starch hydrolysis¹⁰ or polymerization analysis.^{11,12}

In this work, a method based on NIRS and multivariate calibration was developed for the simultaneous monitoring of all components of an esterification reaction, which could be a good model for the monitoring of an industrial process of interest. In this way, the industrial process was simulated at the laboratory level with a view to its subsequent implementation on a production scale.

The selected reaction, the sulfuric acid catalysed esterification of butan-1-ol (BuOH) by acetic acid (AcH), is well established. The reaction is represented by the following scheme:



where AcBu represents *n*-butyl acetate.

The concentration ratio (Q) of this reaction is:

$$Q = \frac{[\text{AcBu}][\text{H}_2\text{O}]}{[\text{AcH}][\text{BuOH}]}$$

which becomes the equilibrium constant (K) once the reaction reaches equilibrium.

Generally, the reaction progress must show increasing product content and decreasing reactant content. For a second-order reaction, the reciprocal of the amount of a reaction component must be directly proportional to the time. For this particular reaction, therefore, the integrated form of its rate equation will be:

$$\frac{1}{[\text{B}]_0 - [\text{A}]_0} \ln \left(\frac{[\text{A}]_0[\text{B}]_t}{[\text{B}]_0[\text{A}]_t} \right) = kt \quad (1)$$

where A_0 and B_0 are the initial concentrations of butan-1-ol and acetic acid, A_t and B_t are the respective concentrations at time t , and k is the rate constant.¹³

Experimental

Apparatus

A Foss NIRSystems 5000 spectrophotometer (FOSS NIRSystems, Silver Spring, MD, USA) fitted with a sample transport module was used to record transmission spectra. The instrument was controlled via the VISION v. 2.21 software package.

A gas chromatograph, Hewlett-Packard (Palo Alto, CA, USA) HP5890, with flame ionization detection (FID) equipped with an HP3396A integrator was used.

The experimental set-up also included a Selecta Agimatic-N heater and Frigitherm thermostated bath (Barcelona, Spain), and a Gilson Minipuls-2 peristaltic pump (Villiers-le-Bel, France).

Catalysed esterification of butan-1-ol by acetic acid

Glacial acetic acid (for analysis, Panreac, Barcelona, Spain), butan-1-ol (for analysis, Panreac) and concentrated sulfuric acid (for analysis, Panreac) were the starting materials. In all, 18 reactions were performed in a 250 ml reaction vessel set in a water-bath, heated and stirred by a thermostated plate. In all cases a fixed amount of butan-1-ol (46 ml, 0.5 mol) was mixed with different amounts of acetic acid (15, 30 and 60 ml corresponding to 0.25, 0.5 and 1 mol), and a related amount of sulfuric acid (1% of the total molar sum) was added as a catalyst. Aliquots of approximately 2 g were withdrawn from the solution at different time intervals to determine butan-1-ol and *n*-butyl acetate using the GC reference method. To preserve the aliquots and stop the reaction before GC determination, sodium carbonate was added to neutralize the sulfuric acid and the aliquots were held at 0 °C.

Laboratory samples

Laboratory samples were prepared by mixing different amounts of glacial acetic acid, butan-1-ol, *n*-butyl acetate (for analysis, Panreac) and doubly distilled water. In all, 52 laboratory

samples, 10 binary, 12 ternary and 30 quaternary, were prepared. Twenty-four of the samples followed the time composition profiles of reactions with initial 2:1, 1:1 and 1:2 (AcH:BuOH) molar ratios. The other 28 were randomly prepared, avoiding the same ratio among analytes as in the reactions to be performed, to decrease correlation among analytes. The molar fraction values of the analytes in these samples were between 0 and 0.7 for acetic acid and butan-1-ol, and between 0 and 0.55 for *n*-butyl acetate and water. All samples were prepared to avoid a common total mass or molar sum. To stop reaction among the analytes before their NIR measurement, samples were held at 0 °C. A GC study proved the stability of the samples throughout the measurement period.

GC reference procedure

The following GC procedure was used as a reference in the determination of butan-1-ol and *n*-butyl acetate. About 2 g of all standards and all aliquots coming from the reactions, which had previously been filtered to remove the excess of sodium carbonate, were mixed with 1 g of isobutyl methyl ketone (IBMK) used as internal standard. The method, which employed a Supelco (Bellefonte, PA, USA) SPB-1 column (30 m × 0.25 mm id, 0.25 µm film thickness), was performed isothermally at 60 °C and samples were injected using a 0.1 µl syringe and a 1:50 split ratio. Mixtures of butan-1-ol and *n*-butyl acetate, with composition values suitable to encompass all the studied cases, were prepared as standards. The ratio between the individual area of the analytes and the area of IBMK was used for the quantification of both analytes.

Recording of NIR spectra

The prepared laboratory samples were circulated at different temperatures, from 20 to 30 °C through a thermostated quartz flow cell of 0.5 mm pathlength (see manifold in Fig. 1) and their spectra recorded as the average of 32 scans over the wavelength range 1100–2500 nm. For reaction monitoring, spectra were recorded at regular time intervals using the same instrumental set-up.

Fig. 2 shows the NIR spectra for acetic acid butan-1-ol, *n*-butyl acetate and water and NIR reaction spectra showing the evolution of the signal with time.

Data processing

Experimental results were processed by using PLS1 and PLS2 partial least-squares (PLS) algorithms included in UNSCRAM-

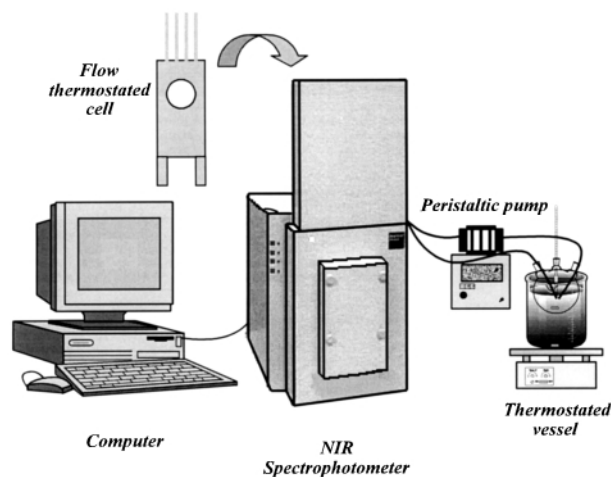


Fig. 1 Experimental system manifold.

BLER v.7.5 from CAMO (Trondheim, Norway). Calibration models were constructed by cross-validation, using as many segments as samples employed for calibration (leave-one-out procedure). The number of significant PLS components was estimated on the basis of the criterion of Haaland and Thomas.¹⁴ Derivative transformation was performed using the Savitzky–Golay method (polynomial order 2 and window 6) implemented in UNSCRAMBLER.

The quality of the results was assessed in terms of the relative standard error of prediction, RSEP(%).¹⁵

Results and discussion

As is evident from Fig. 2, there is a large degree of correlation between the intensity of some bands and the reaction evolution, which causes a band intensity growth in the ranges 1400–1450 and 1900–1950 nm, which correspond to the first overtone and combination bands of O–H water bonds, respectively, and a decrease in the ranges 1650–1800, 2050–2100 and 2200–2450 nm, which correspond to the C–H first overtone, RO–H and C–H combination bands, respectively. It is well known that the exact shape and location of O–H absorption bands is dependent on the number of hydrogen bonds, which are strongly temperature-dependent.¹⁶ To obtain an idea of this influence in the studied spectra, difference spectra between measurements of the same samples at different temperatures (from 20 to 60 °C) were calculated, and showed no differences except for the O–H bands, which presented a slight shift and an intensity difference equivalent to 1% of the initial spectral values in absorbance units. Owing to this minimum variation and to facilitate the experimental procedure, initially it was decided to measure spectra of laboratory samples at ambient temperature, ranging from 20 to 30 °C, even though reactions were measured at higher temperatures in order to achieve equilibrium in a reasonable period of time.

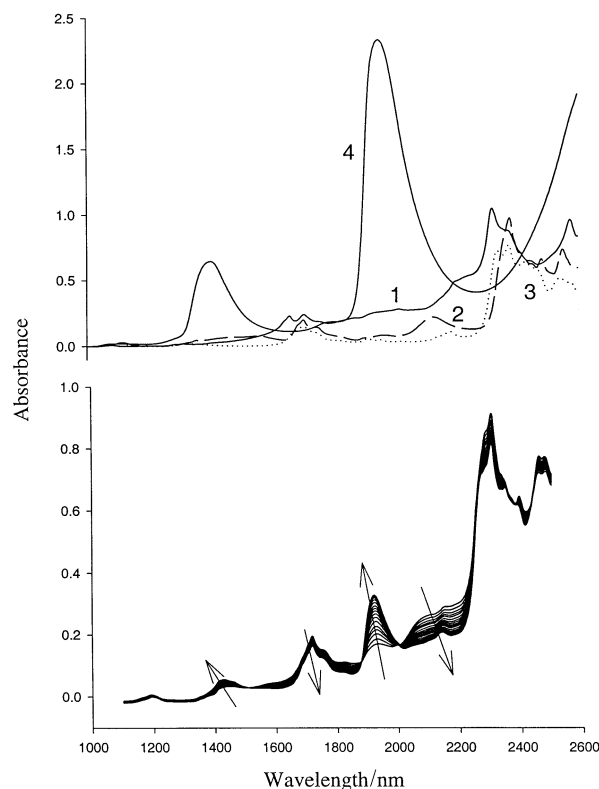


Fig. 2 Top: NIR spectra for (1) acetic acid, (2) butan-1-ol, (3) *n*-butyl acetate and (4) water. Bottom: NIR reaction spectra showing the evolution of the signal with time.

As the reaction proceeds, the formation of water and butyl acetate changes the polarity of the medium, which causes a dispersion in the reaction samples and leads to a baseline shift of the spectra. The acetic acid helps to keep water and butyl acetate in the same phase; however, a second phase appears when performing the reaction with acetic acid as a minority reagent and after only 2 h of reaction. This baseline causes significant errors in the prediction of water but, due to the second-derivative pre-treatment, it does not affect the results of the main studied species. In any case, at this point the reaction is almost complete and the information can be removed. Moreover, the sodium carbonate added to the reacting samples in order to neutralize the sulfuric acid and stop the reaction partially reacts with the acetic acid, especially as the reaction proceeds and the medium becomes more polar. This prevents the correct determination of acetic acid by the GC method.

The reaction was studied without any solvent; therefore, molar fractions were selected as units, which means that the total molar fraction sum should always be the same as the reactions proceed.

In this work, a set of externally prepared samples were used to construct the calibration models. A calibration set consisting of solutions containing the products present during the process, *viz.* the starting acetic acid and butan-1-ol and the formed *n*-butyl acetate and water, was prepared.

PLS models were constructed by splitting the 52 initial laboratory samples into a calibration sub-set (28 samples) and an external validation set (24 samples); the latter was used to determine predictive capacity. The samples for inclusion in each set were selected in such a way that they would span the concentration range for each parameter. Correlation among analytes was always less than 0.4, avoiding the characteristic correlation when using only reacting samples.

One important requirement when constructing the calibration method is to select an appropriate wavelength range. Various spectral ranges were tested: first, the full spectrum was tested and, subsequently, regions where the quantified components exhibited a low absorption were excluded from the calculations. Calibration models were thus constructed for each parameter to be determined (AcH, BuOH, AcBu and H₂O), using different wavelength intervals in the absorbance, and first- and second-derivative modes. The best models obtained are shown in Table 1. The simplest and most suitable were those involving the wavelength range 1600–2500 nm for acetic acid and *n*-butyl acetate and 1300–2500 nm for butan-1-ol and water, which fitted with the elimination of negligible absorbing regions (Fig. 2).

The results obtained for each parameter were very similar in all spectral models; however, the number of principal components was smaller with the derivative modes and corresponded better with the number of analytes, four. The derivative modes offset baseline shifts and drift arising from a small dispersion of water and *n*-butyl acetate in the solutions. The relative standard error of prediction, RSEP, was slightly better in the second-derivative mode, less than 1.7% in all cases.

As there were four analytes to determine, various models based on the PLS2 algorithm for calibration were tested. The most suitable model was found to be that using four PLS components and the wavelength range from 1300 to 2500 nm in the second-derivative mode. The RSEP values found (Table 2) were comparable to those obtained by individual PLS1 models.

Esterification

The previously constructed models were used to monitor the esterification of butan-1-ol by acetic acid.

A 3² full factorial design consisting of two factors at three different levels: initial AcH:BuOH molar ratio (2:1, 1:1 and

1:2) and temperature (40, 50 and 60 °C), was used as conditions for the reaction. In all, 18 reactions were performed nine corresponding to the design and nine replicates.

The spectra recorded during esterification experiments were quantified using the models constructed previously. Simultaneously with the spectral recordings, aliquots were withdrawn from the samples for analysis by the GC method. RSEP values (Tables 1 and 2) were clearly lower using the second-derivative mode and were always less than 3.5%. These values are higher than those obtained for laboratory samples, but are perfectly acceptable in a control analysis. This difference was because the laboratory and reaction samples had different reference methods; in the former, reference values came from weight values, and in the latter, from GC. Another cause could be the effect on the spectra of the occurrence of dispersion at the end of some reactions, which was partially corrected by performing second-derivative measurements. Moreover, RSEP values strongly depend on the magnitude of the studied variable; hence, similar absolute errors lead to different RSEP values, especially when using values near or equal to zero, which is the case for the studied reactions, especially for *n*-butyl acetate.

A PLS2 model was selected as the simplest and best model to perform the determination. As can be seen in Fig. 3, a good concordance between NIR predicted values and GC reference values was obtained using the PLS2 model; also, the figures of merit of the curves reveal the absence of systematic errors (slopes and intercepts are not significantly different from unity and zero, respectively, for both butan-1-ol and *n*-butyl acetate). The dotted lines show a 0.025 margin in molar fraction units; as can be seen, all samples are within these margins which confirms the suitability of the method at any point of the studied ranges. It is important to mention that the constructed model was suitable at higher temperature (40–60 °C) than those used in calibration (20–30 °C), which avoided the need to measure more laboratory samples at higher temperatures and fitted with the initial estimation made about the influence of temperature. A statistical study revealed the absence of correlation between the temperature and the absolute error of prediction values, thus confirming the absence of systematic errors arising from changes in temperature.

Fig. 4 shows, as an example, the reaction profiles predicted for an esterification reaction performed at 50 °C; as can be seen, prediction curves for butan-1-ol and *n*-butyl acetate fitted very well with the GC values. Even though we did not have reference

values for acetic acid and water, in reactions with identical initial values for both reagents, predicted acetic acid and water curves were the same as for butan-1-ol and *n*-butyl acetate, respectively. Moreover, the sum of all molar fractions was

Table 2 Relative standard error of prediction calculated for the calibration set (RSEPC) and prediction sets RSEPP₁ (laboratory samples) and RSEPP₂ (reaction samples) for the best PLS2 model (second-derivative, four PLS components, 1300–2500 nm) using molar fraction (Xs) and % mass (% m/m) as predictors

Analyte	PLS2					
	Laboratory samples				Reaction samples	
	RSEPC (%)		RSEPP ₁ (%)		RSEPP ₂ (%)	
	Xs	% m/m	Xs	% m/m	Xs	% m/m
AcH	0.79	0.64	1.39	1.83	—	—
BuOH	0.48	0.54	0.53	0.63	1.72	1.76
AcBu	1.21	1.44	1.61	1.58	3.47	3.31
H ₂ O	1.37	0.67	1.66	0.97	—	—

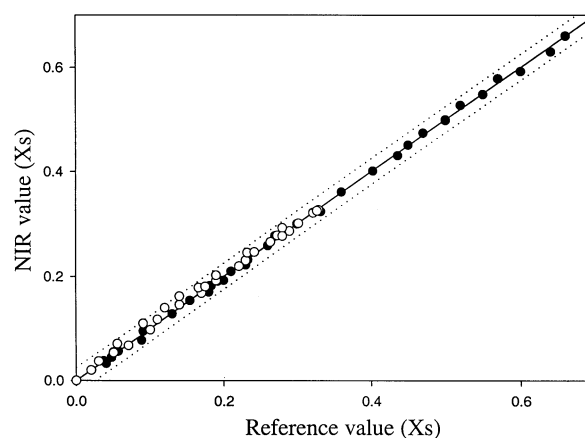


Fig. 3 Plot of butan-1-ol and *n*-butyl acetate NIR predicted values (expressed as a molar fraction) in relation to the GC reference values. The dotted lines show a 0.025 margin in molar fraction units. (●) BuOH (○) AcBu. Figures of merit: BuOH (intercept = -0.002 ± 0.006 , slope = 1.003 ± 0.007 , $r = 0.999$); AcBu (intercept = -0.008 ± 0.009 , slope = 0.98 ± 0.03 , $r = 0.998$).

Table 1 Relative standard error of prediction calculated for the calibration set (RSEPC) and prediction sets RSEPP₁ (laboratory samples) and RSEPP₂ (reaction samples) for the best PLS models in acetic acid, butan-1-ol, butyl acetate and water calibrations

PLS1						
Spectral range/nm	Spectral mode	PLS components	Laboratory samples		Reaction samples	
			RSEPC (%)	RSEPP ₁ (%)	RSEPP ₂ (%)	
AcH— 1600–2500	Absorbance	5	1.14	1.69	—	
	First-derivative	4	0.79	1.24	—	
	Second-derivative	4	0.74	1.04	—	
BuOH— 1300–2500	Absorbance	5	0.98	1.16	5.21	
	First-derivative	4	0.74	1.14	3.88	
	Second-derivative	4	0.74	0.98	1.50	
AcBu— 1600–2500	Absorbance	5	0.72	2.14	7.35	
	First-derivative	4	0.72	1.97	5.26	
	Second-derivative	4	0.62	1.61	3.26	
H ₂ O— 1600–2500	Absorbance	5	1.16	2.21	—	
	First-derivative	4	1.10	1.96	—	
	Second-derivative	4	0.98	1.47	—	

always equal to 1 ± 0.01 , confirming the suitability of the model for acetic acid and water also.

Replicates, which showed almost identical reaction profiles, proved the reproducibility of the proposed method.

So far, reaction profiles have been predicted and plotted and have shown a good correlation with the reference method. However, the profiles should also follow second-order reaction kinetics.

Kinetic plots were generated by plotting the integrated form shown in eqn. (1) vs. time. As can be seen in Fig. 5, which corresponds to the kinetic plots for the reactions performed at 60, 50 and 40 °C with an initial 2:1 AcH:BuOH molar ratio, the relationship is not linear, especially at the end of the reaction. The slopes of linear least-squares lines fitted to ten-point windows throughout the course of the reaction showed that, as expected, the formation of the product occurred at a faster rate at the beginning of the reaction, becoming slower as the reaction proceeded. This effect could be explained in terms of changes in the composition of the reaction medium as the reaction progressed, which limited the kinetic study to the beginning of the reaction, allowing only estimations of initial rate constants to be made (using only the first ten points of each reaction). The characteristics of the used design allowed a statistical study to be performed based on a two-way analysis of variance (ANOVA), which demonstrated a significant influence of both factors, *viz.*, temperature and initial reagents ratio, and their interaction, on the found rate constants. Moreover, as tem-

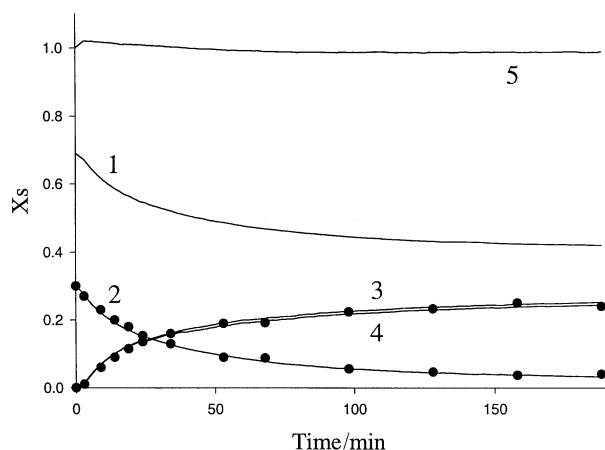


Fig. 4 Reaction profiles for (1) acetic acid, (2) butan-1-ol, (3) *n*-butyl acetate, (4) water and (5) total sum, during esterification at 50 °C and an initial 2:1 molar ratio. The solid lines show the NIR predicted values and the symbols (●) show the GC values found.

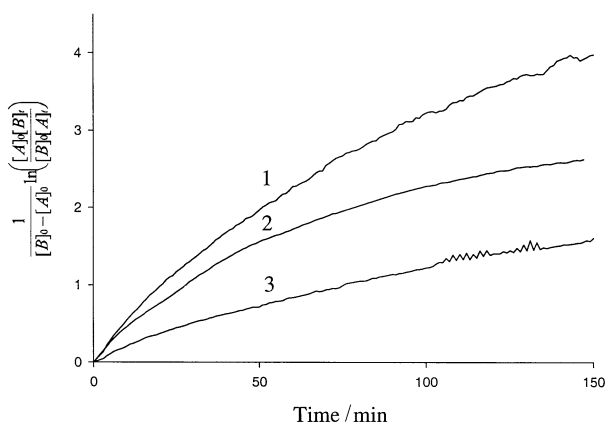


Fig. 5 Kinetic plot of reactions performed at (1) 60, (2) 50 and (3) 40 °C and an initial 2:1 AcH:BuOH molar ratio, showing the relationship between the integrated form of a second-order reaction vs. time.

perature was one of the studied factors, an evaluation of activation energies could be performed. As can be seen in Table 3, where the rate constants as well as the activation energies found for all cases are shown, the fastest reaction was that performed at 60 °C with an initial 2:1 molar ratio of AcH:BuOH; also, there is an important difference in terms of activation energy between reactions performed with large amounts of starting acetic acid and those that are not, which could be explained in terms of autocatalysis of the acetic acid H^+ .

To determine the equilibrium-point of the reaction, the concentration ratio (Q) was calculated at every time from the predicted values. As can be seen in Fig. 6, when the reaction achieves equilibrium, the line becomes constant giving the end-point and an approximation of the equilibrium constant (K_{eq}). All reactions performed at the same temperature led to the same K_{eq} .

In order to check the importance to the performance of the reaction of the initial water contamination, which could come mainly from the acetic acid, two new experiments were performed by initially adding 2 and 5% v/v water to the most favourable case, *viz.* 2:1 at 60 °C. As can be seen in Fig. 6, the addition of 5% water caused a significant decrease in the initial slope of the reaction and retarded the achievement of equilibrium, while in the 2% case differences were minimal. As expected, all cases led to the same equilibrium constant.

To prove the suitability of the proposed methodology, the best model conditions found, *viz.* PLS2, were tested by changing the variable units to % m/m. As the calibration samples were prepared to avoid an equal sum of mass or moles, there was no relation between the two units, molar fraction and m/m, and hence the related model should not be equal. As can

Table 3 Rate constants and activation energies (E_a) found in the studied esterification design and its replicates

Temperature/°C	Rate constant/s ⁻¹			E_a /kJ mol ⁻¹
	Initial molar ratio AcH:BuOH			
	2:1	1:1	1:2	
40	0.058	0.052	0.004	133
	0.057	0.051	0.006	
50	0.084	0.078	0.062	44
	0.082	0.079	0.064	
60	0.151	0.142	0.085	41
	0.151	0.143	0.084	

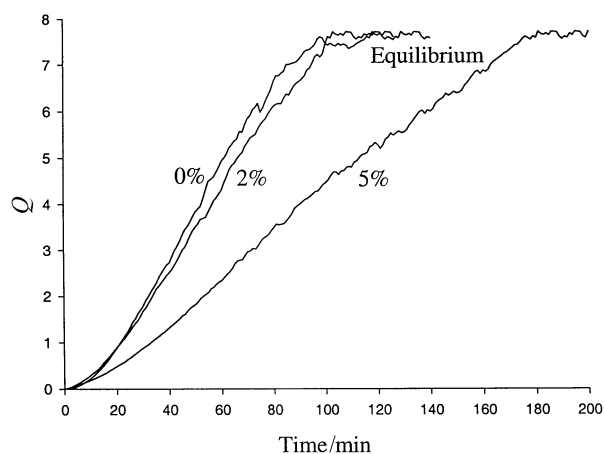


Fig. 6 Concentration ratio (Q) profiles for the most favourable case, 2:1 at 60 °C, with the estimation of the equilibrium-point, and comparison with the same case but adding an initial 2 and 5% v/v water to the acetic acid.

be seen in Table 2, comparable results to the former results were found.

Finally, as a more usual industrial way of following alcohols in esterification processes is by using the hydroxyl number (mg g^{-1} KOH), the calibration model for BuOH was reconstructed using this variable RSEPP, values less than 1.5% were found for both laboratory and reaction samples.

Conclusions

An NIR method is proposed as an alternative to the labour-intensive chromatographic methods for monitoring an esterification, which allows the simultaneous determination of all the involved species using a single model. The NIR predicted values are consistent with those provided by the reference method.

The use of calibration with external samples facilitates implementation of the method and avoids the characteristic correlation among analytes when samples taken from dynamic systems are used. The constructed model has a good predictive behaviour even with samples measured at higher temperatures than those used for calibration, which simplifies significantly the calibration process.

Studies were made to prove the concordance of the method with second-order reaction kinetics. The usefulness of the proposed NIR method to determine rate constants, equilibrium-points and the effect of initial impurities was also demonstrated.

The used experimental design showed that the most favourable case was that using a higher temperature and an excess of acetic acid, and proved the significance of the studied factors, temperature and initial reagents ratio, in the performance of the reaction.

Although the method developed was used in laboratory-scale experiments, the simplicity and expeditiousness with which the reaction can be determined makes the proposed method

potentially useful for monitoring full-scale industrial esterification processes also.

Acknowledgements

The authors are grateful to the DGICYT, Spain, for funding this work, as part of project PB96-1180. Daniel Serrano also acknowledges additional support from the DGU of the Generalitat de Catalunya in the form of a scholarship.

References

- 1 S. Wold, N. Kettaneh, H. Friden and A. Holmberg, *Chemom. Intell. Lab. Syst.*, 1998, **44**, 331.
- 2 K. S. Dahl, M. J. Piovoso and K. A. Kosanovich, *Chemom. Intell. Lab. Syst.*, 1999, **45**, 199.
- 3 C. Coffey, B. E. Cooley and D. S. Walker, *Anal. Chim. Acta*, 1999, **395**, 335.
- 4 B. G. Osborne and T. Fearn, *Near Infrared Spectroscopy in Food Analysis*, Longman Scientific and Technical, New York, 1986.
- 5 M. Blanco, J. Coello, H. Iturriaga, S. MasPOCH and C. de la Pezuela, *Analyst*, 1998, **123**, 135R.
- 6 S. J. Swarin and C. A. Drumm, *Spectroscopy*, 1992, **7**, 42.
- 7 H. M. Heise, A. Bitmer and R. Marbach, *J. Near Infrared Spectrosc.*, 1998, **6**, 349.
- 8 A. Cavinato, D. M. Mayes, Z. Ge and J. B. Callis, *Anal. Chem.*, 1990, **62**, 1977.
- 9 G. Büttner, *Process Control Quality*, 1997, **9**, 197.
- 10 M. Blanco, J. Coello, H. Iturriaga, S. MasPOCH and R. González Bañó, *Analyst*, 2000, **125**, 749.
- 11 R. Heikka, K. T. Immonen, P. O. Minkkinen, E. Y. O. Paatero and T. O. Salmi, *Anal. Chim. Acta*, 1997, **349**, 287.
- 12 R. Mackison, S. J. Brinkworth, R. M. Belchamber, R. E. Aries, D. J. Cutler, C. Delley and H. Mould, *Appl. Spectrosc.*, 1992, **46**, 1020.
- 13 P. W. Atkins, *Physical Chemistry*, Oxford University Press, Oxford, 4th edn., 1990, p. 786.
- 14 D. M. Haaland and E. V. Thomas, *Anal. Chem.*, 1988, **60**, 1193.
- 15 M. Otto and W. Wegscheider, *Anal. Chem.*, 1985, **57**, 63.
- 16 J. N. Finch and E. R. Lippincott, *J. Phys. Chem.*, 1957, **61**, 894.